From Homogeneous to Heterogeneous Nucleation of Chain Molecules under Nanoscopic Cylindrical Confinement

Euntaek Woo,[1] June Huh,[2] Young Gyu Jeong,[3] and Kyusoon Shin[1,*]

[1]*School of Chemical and Biological Engineering, Seoul National University, Seoul 151-742, South Korea*

[2]*Hyperstructured Organic Materials Research Center and School of Materials Science and Engineering, Seoul National University, Seoul 151-742, South Korea*

[3]*School of Advanced Materials and Systems Engineering, Kumoh National Institute of Technology, Gumi 730-701, South Korea*

(Received 9 October 2006; published 28 March 2007)

The crystallization of monodisperse linear polyethylene confined in nanoporous alumina is investigated with the calorimetric measurements. We observe a drastic change in crystallization behavior, specifically nucleation, with a decrease in the pore diameter. Crystallization in relatively larger pores with the diameters of 62 and 110 nm occurs at lower temperatures within a very narrow range, whereas crystallization in smaller pores with diameters of 15–48 nm occurs at a higher and broad range of temperatures. Nucleation and crystallization kinetics in nanopores is discussed based on classical nucleation theory as well as the Avrami theory.

DOI: 10.1103/PhysRevLett.98.136103 PACS numbers: 81.07.−b, 81.10.Aj, 81.10.Fq, 82.35.Lr

Physical properties of materials which are well defined and clearly fixed in the bulk are very often no longer typical features in the nanometer scale. For instance, nanocrystals show size-dependent properties such as fluorescence [1] and melting point depression [2]. Many useful optical and electronic properties of nanocrystals are tunable without much difficulty nowadays as the shape and size can be controlled via various synthetic methods [3–5]. Realizing that several important physical properties are governed by crystal structures, the understanding of crystallization kinetics in nanoscopically confined spaces is of crucial importance for developing novel nanomaterials that exhibit various nontraditional properties.

Crystalline polymers are of particular interest due to their tendency to form in bulk nanoscopic and highly anisotropic structures [6]. Once the anisotropic crystalline structures meet another nanoscopic geometry, for example, one-dimensional cylindrical nanostructure [7,8], those combined multiple-length scale structures could be used as high density electronic devices without deteriorating their original properties [5]. Under the geometry of nanoscopic confinement, the crystallization behavior of polymers must be strongly perturbed. Some of the previous studies have focused mostly on the structure and crystallization behavior of polymers under one-, two-, or three-dimensional confinement, revealing the details of the crystal structure in conjunction with geometric features of confinement [7–12]. Although those results enable us to speculate the mechanism of polymer crystallization under a strongly confined condition, the understanding of kinetics is still limited due to the difficulty in direct measurement of crystal growth over a broad range of confinement geometries.

In this Letter, we report the crystallization kinetics of monodisperse linear polyethylene (PE) in nanoporous alumina and show that the kinetic behavior is drastically altered as the diameter of cylinders becomes smaller. The pore diameter is varied over a wide range from a small dimension comparable to the nucleus size to several times of repeating period of lamellar crystal in bulk. Thus, we expect that the nanoscopic cylindrical confinement imposed on the polymer chains induces significant alteration of nuclei formation or crystallite growth. In this system, both ends of the PE chain are free to move, and the anodic alumina template provides the well-defined cylindrical nanopores which are regularly sized, straight, and linear all the way through [13]. The thermal and mechanical rigidity of alumina avoids the breakdown of nanoscopic confinement due to crystal growth [14]. The use of fractionated linear PE detours the potential effect of broad molecular weight distribution and short chain branches on the main chain crystallization [15].

The alumina membranes with regular pore diameters were fabricated via the two-step anodization [13]. Fractionated monodisperse linear PE was purchased from NIST (Standard Reference Material® 1483a, $M_w =$ 32 100 g/mol, $M_w/M_n = 1.11$). The sample preparation is schematically shown in Fig. 1. Bilayer films consisting of a PE top layer and a polystyrene (PS, $M_w =$ 280 kg/mol, Aldrich Chemical, Co.) bottom layer were prepared by solution casting on glass substrates and followed by detaching and overlaying the PE film on the

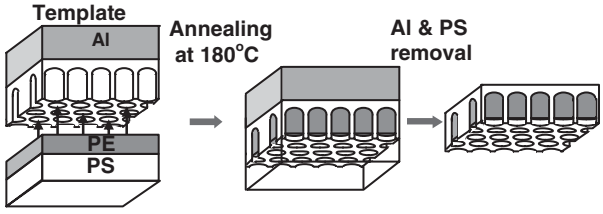

FIG. 1. Schematic illustration of sample preparation.

supporting PS film. The nanopores were filled with the linear PE by annealing the film and alumina membrane assembly in a vacuum oven at 180 °C for more than 5 days. After annealing, the remaining aluminum and PS were removed by dissolving in cupric chloride solution [16] and toluene, respectively. Since PE film was not thick enough to fill the pore completely, PE was located only in the pore after removing PS. The isothermal crystallization experiments of the linear PE in nanopores were carried out on a Perkin-Elmer DSC7 equipped with a refrigerating cooler. The weights of linear PE were calculated based on the thicknesses of initial linear PE films and the total area of the membranes in the pan. The isothermal crystallization experiment was carried out by heating each sample to 180 °C, holding for 10 min to erase the thermal history, cooling to predetermined crystallization temperature (T_c) at a rate of 100 K/ min, and holding for crystallization.

The kinetics of crystallization follows the Avrami equation, $1 - X_c = \exp(-Kt^n)$ [17]. Here, X_c is the relative crystallinity at a specific time t. K and the exponent n are referred to as Avrami constants. The isothermal crystallization kinetics of the linear PE confined in the nanocylinders was analyzed by Avrami theory to get the information on the contribution of nucleation and growth. The experimental parameters and Avrami constants are summarized in Table I. It is noteworthy that the n values ($n = 1.6$–1.9) of linear PE crystallization in the nanocylinders are smaller than the one ($n = 2.4$) obtained from the crystallization in bulk. The exponent n is known to be dependent on growth geometry and the crystallization mechanism [17]. Crystallization of PE in bulk is known to be initiated by the heterogeneous nucleation with a relatively small number density of nuclei and followed by the dominant three-dimensional spherulitic growth [18]. The cylindrical constraint geometry and limited volume of the nanoporous alumina give rise to the frustration of crystal growth. Therefore, nucleation is dominant, leading to the reduced Avrami exponent n for the crystallization in the cylindrical geometry. The decrease in n values has been reported for the crystallization in thin polymer films [10] as well as in the spherical microdomains of semicrystalline-amorphous diblock copolymer [11], and the dominating nucleation was suggested to be responsible for this decrease. Similarly, in the cylindrical nanopores, the nucleation is the major contribution to overall crystallization.

Crystallization in the nanopores occurs at lower T_c(<99 °C), compared with the bulk crystallization (T_c = 114–122 °C), as listed in Table I. Since nucleation is dominant in the nanopores and the nucleation rate is higher at lower T_c in general [18], the exotherms for the crystallization in the nanopores are observed only at lower T_cs. At higher T_cs, crystallization in nanopores is not discernible presumably due to the small number density of nuclei and restricted crystal growth. Overall, the decrement of T_c for the crystallization in nanopores indicates that the nucleation is dominant over the crystal growth.

The Avrami constant K, depicting the contribution of the crystal growth rate, the nucleation rate, and the number of nuclei, is 6 orders of magnitude larger in the nanocylinders than that in the bulk (Table I). With the above information of the suppressed crystal growth in the pores, the significant increase in K, as compared to that in bulk, suggests a larger number of nuclei or higher nucleation rates in the nucleation of PE in nanopores. The reciprocal of crystallization halftime ($t_{1/2}^{-1}$), a measure of crystallization rate of PE in nanopores and in bulk, is plotted in Fig. 2 as a function of T_c (lower axis) and ΔT (upper axis). Here, $t_{1/2}$ is the time at which the crystallinity reaches half of the finally attained value at each T_c, and ΔT is the degree-of-supercooling, the difference between the equilibrium melting temperature (T_m°, 146.5 °C for linear PE [19]) and T_c. It is found from the slopes shown in Fig. 2 that the crystallization behavior of PE is appreciably affected by the existence of confinement. The crystallization rates in the nanopores with the diameters of 62 and 110 nm are significantly dependent on the crystallization temperature, compared with those in the bulk. The slope for the bulk crystallization is -1.37×10^{-2} sec^{-1} K^{-1}, while those are -4.08×10^{-2} and -3.26×10^{-2} for crystallization in the 62 and 110 nm pores, respectively. On the other hand, it is noteworthy that the crystallization rates of PEs in the 15–48 nm pores exhibit very weak tempera-

TABLE I. Avrami constants obtained from the isothermal crystallization of linear PE in pores and in the bulk.

Samples		T_c range (°C)	n	K
In nanopores (pore diameter, nm)	15	75–99	1.7 ± 0.1	4.1×10^{-2}
	20	75–99	1.7 ± 0.1	4.1×10^{-2}
	33	75–99	1.6 ± 0.1	3.6×10^{-2}
	41	75–99	1.7 ± 0.1	2.6×10^{-2}
	48	75–99	1.7 ± 0.2	2.9×10^{-2}
	62	80–84	1.9 ± 0.1	1.0×10^{-2}
	110	79–83	1.9 ± 0.1	0.8×10^{-2}
In bulk		114–122	2.4 ± 0.2	3.7×10^{-8}

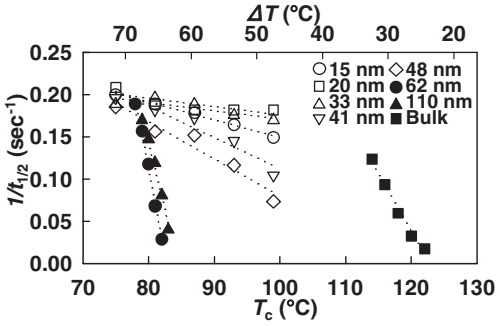

FIG. 2. Crystallization rate ($1/t_{1/2}$) as a function of the crystallization temperature (T_c) or the degree-of-supercooling (ΔT).

ture dependence, unlike in 62 and 110 nm pores. When the diameter is smaller than 48 nm, the slopes suddenly become smaller by 1 or 2 orders (-0.1 to -4.4×10^{-3}) than those for larger pores. The T_c ranges also vary abruptly between 48 and 62 nm pores. The crystallization in the 62 and 110 nm pores occurs at lower and narrower T_c ranges ($\Delta T \sim 65\,^{\circ}\mathrm{C}$) than in the smaller 15–48 nm pores. We observed crystallization exotherms on broad ranges of temperatures, even at $T_c = 99\,^{\circ}\mathrm{C}$ (or $\Delta T = 47.5\,^{\circ}\mathrm{C}$), in 15–48 nm pores.

As mentioned earlier, crystallization in the nanopores is governed by nucleation rather than crystal growth. Hence, the confinement dimension-dependent crystallization kinetics can be explained in view of nucleation mechanism. In the cases of 62 and 110 nm pores, large ΔT ($\sim 65\,^{\circ}\mathrm{C}$) and steep temperature dependence of $t_{1/2}^{-1}$ (Fig. 2) supports the fact that the overall crystallization of PE in those pores is governed by homogeneous nucleation. Homogeneous nucleation, initiated without any assistance of foreign objects, is known to require larger critical nucleus size (few to tens of nanometers along the direction of chain axis), and therefore it occurs at ΔTs larger than that for the heterogeneous nucleation [18]. Additionally, the homogeneous nucleation rate depends more strongly on the temperature than heterogeneous nucleation because there is no free energy gain due to the absence of any preexisting surface to the nucleus formation [18]. The large ΔT and steep temperature dependence of $t_{1/2}^{-1}$ has been also reported for other homogeneous nucleation-dominant systems such as micron-sized polymer droplet [20,21] or crystalline-amorphous diblock copolymer [11].

In the smaller pores with diameters of 15–48 nm, the crystallization behavior of PE is different from the one in larger pores in that crystallization occurs at smaller ΔT with a very weak temperature dependence. It implicates that heterogeneous nucleation dominates the overall crystallization of PE in the pores with diameters of 15–48 nm. According to the classical concept on crystal nucleation, a nucleus is stable only when its dimension is larger than the critical nucleus size [18]. For heterogeneous nucleation, the critical nucleus size is predicted to be proportional to $\sim\Delta\gamma$ (the surface free energy difference between the nucleus and preexisting substrate) and $\sim\Delta T^{-1}$ [18]. The critical nucleus size is almost unaffected by the temperature at large ΔTs since the critical nucleus cannot be smaller than the molecular scale and $\Delta\gamma$ is also small. Therefore, in heterogeneous nucleation, the nucleation rate is almost independent of the temperature at sufficiently low T_c [18]. In the bulk, crystal growth contributes mainly to the overall crystallization kinetics, compared with heterogeneous nucleation [18], and the crystallization rate depends on ΔT appreciably. On the other hand, in the smaller 15–48 nm pores, nucleation governs the overall kinetics because of the geometrical limitation on crystal growth. Therefore, the very weak temperature dependence of $t_{1/2}$ means that heterogeneous nucleation is a dominant contribution to the overall crystallization. As the pore diameter decreases, the surface-to-volume ratio increases, and the polymer chain is likely to have more chances of forming a nucleus from the surface of nanopores. However, the slopes of the $33 \sim 48$ nm diameter pores in Fig. 2 are slightly larger than those of 15 and 20 nm pores. It is thought that there is minor contribution of homogeneous nucleation in the intermediate-sized pores.

Assuming that regular sized crystallites are formed, the nucleation in the larger nanopores is similar to droplet-type homogeneous nucleation [20,21]. According to nucleation theory, the $t_{1/2}$ of a homogeneous nucleation-dominant system is related to the T_c as follows [18];

$$\ln t_{1/2} = \text{const} + \frac{32\gamma^2\gamma_e T_m^{\circ 2}}{k(\Delta h_f \rho_c)^2}\frac{1}{T_c \Delta T^2}, \qquad (1)$$

where Δh_f is the bulk free enthalpy of the crystal and ρ_c is the density of the crystal. γ and γ_e are the lateral and fold surface free energies of a nucleus, respectively. With the information of $\Delta h_f = 2.9 \times 10^2$ J/g and $\rho_c = 1.0$ g/cm^3 [18], we can calculate the surface energy product ($\gamma^2\gamma_e$) from the slope of the semilogarithmic plot of $t_{1/2}$ versus $1/T_c\Delta T^2$, as shown in Fig. 3. The $\gamma^2\gamma_e$ values are evaluated to be 8.2×10^{-6} and 6.0×10^{-6} J^3/m^6 for 62 and 110 nm diameter pores, respectively. These values are in reasonable accordance with those obtained from the polymer droplet experiments [22]. The small difference ($\sim 20\%$) is thought to stem from the geometry of the confinement. Since the cylindrical nanopore is a two-dimensionally confined system, crystallization in the nanocylinders in this study is different from the perfectly isolated homogeneous nucleation system such as the crystallization within polymer droplets [22]. The connectivity along the pore axis may induce self-nucleation from preexisting crystals [23,24].

We can also calculate the dimension of critical nucleus from the above crystallization experiments. The longitudinal dimension of critical nucleus (l^*) is expressed by the following equation:[18];

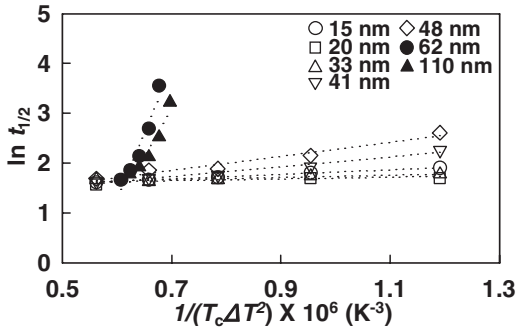

FIG. 3. Crystallization halftime ($t_{1/2}$) as a function of supercooling ($1/T_c\Delta T^2$) in the isothermal crystallization experiment.

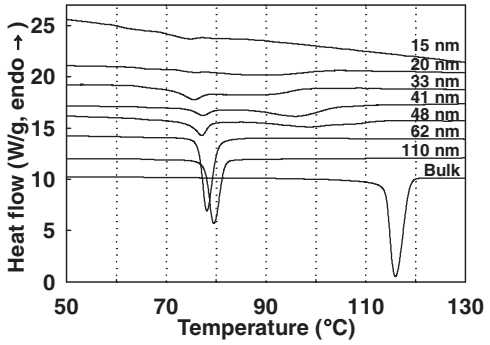

FIG. 4. Cooling thermograms of monodisperse linear PE in the nanoporous alumina with the diameters of 15–110 nm and in bulk. The cooling rate was controlled to be -10 K/ min.

$$l^* = \frac{4\gamma_e T_m}{\Delta h_f \Delta T \rho_c}. \quad (2)$$

Using the γ of 1.0×10^{-2} J/m^2 [18] and the $\gamma^2\gamma_e$ values above, the l^* values are calculated to be 7 and 5.3 nm for the crystals developed in the 62 and 110 nm nanopores, respectively. However, the calculated l^* of crystals developed in the pores with the diameters of 15–48 nm strongly suggests that the homogeneous nucleation in those small pores is not likely to happen. The l^* for those smaller pores with the diameter of 15–48 nm is calculated to be smaller than 1 nm. These values are too small to be the size of a nucleus. Therefore, the homogeneous nucleation theory is not applicable any more as the nucleation mechanism in those 15–48 nm nanopores. The instability of the nucleus developed by homogeneous nucleation in the smaller nanopore must be one of origin of the predominant heterogeneous nucleation in the smaller pores.

The change in nucleation mechanism with the pore diameter can also be observed from the nonisothermal crystallization of PE in the nanopores. DSC thermograms of the samples obtained at the cooling rate of -10 K/ min are shown in Fig. 4. Sharp exothermic crystallization peaks around 80 °C are observed when the pore diameters are 62 and 110 nm. On the other hand, broad peaks covering 60 to 110 °C are detected when the diameters are 15–48 nm. It is interesting that, for 33 and 48 nm pores, a relatively small and sharp peak is also observed with broad exotherm, indicating partial contribution of homogeneous nucleation in addition to the dominant heterogeneous nucleation in those intermediate-sized nanopores. Those temperature ranges for nonisothermal crystallization in the smaller nanopores are consistent with the T_c ranges of the above isothermal crystallization experiments. The nonisothermal crystallization of PE in the bulk consists of heterogeneous nucleation and subsequent crystal growth which occurs just below the melting temperature [18]. The entire crystallization process of heterogeneous nucleation and crystal growth in the bulk occurs within relatively narrow temperature ranges. In the larger pores with the diameters of 62 and 110 nm, however, the homogeneous nucleation is predominant and sharp exotherms are observed at lower temperatures (75 ~ 85 °C) than in the bulk (~ 117 °C). In the smaller pores with the diameters of 15–48 nm, the heterogeneous nucleation prevails, and the crystallization occurs over much wider temperature ranges (60 ~ 110 °C).

In summary, we have investigated the nucleation-governing crystallization of monodisperse linear PE frustrated under the nanoscopic cylindrical confinement. We found from the calculations based on the classical nucleation theory that homogeneous nucleation dominates in larger pores, whereas heterogeneous nucleation prevails in smaller pores.

E. W. and K. S. appreciate the support by the Korean Government (No. KRF-2006-331-D00160, No. R01-2006-000-10749-0).

*Electronic address: shin@snu.ac.kr

[1] M. Nirmal *et al.*, Nature (London) **383**, 802 (1996).
[2] S. L. Lai *et al.*, Phys. Rev. Lett. **77**, 99 (1996).
[3] V. L. Colvin, M. C. Schlamp, and A. P. Alivisatos, Nature (London) **370**, 354 (1994).
[4] C. B. Murray, C. R. Kagan, and M. G. Bawendi, Annu. Rev. Mater. Sci. **30**, 545 (2000).
[5] T. Thurn-Albrecht *et al.*, Science **290**, 2126 (2000).
[6] G. Strobl, *The Physics of Polymers* (Springer, Berlin, 1996), Vol. 1, pp. 143.
[7] M. Steinhart *et al.*, Macromolecules **36**, 3646 (2003).
[8] M. Steinhart *et al.*, Phys. Rev. Lett. **97**, 027801 (2006).
[9] T. Matsuda *et al.*, Macromolecules **28**, 165 (1995).
[10] M. M. Despotopoulou *et al.*, Macromolecules **29**, 5797 (1996).
[11] Y. L. Loo, R. A. Register, and A. J. Ryan, Phys. Rev. Lett. **84**, 4120 (2000).
[12] L. Zhu *et al.*, J. Am. Chem. Soc. **122**, 5957 (2000).
[13] H. Masuda and K. Fukuda, Science **268**, 1466 (1995).
[14] Y. L. Loo, R. A. Register, and A. J. Ryan, Macromolecules **35**, 2365 (2002).
[15] J. Rhee and B. Crist, Macromolecules **24**, 5663 (1991).
[16] Y. M. Sun *et al.*, Macromol. Rapid Commun. **26**, 369 (2005).
[17] M. Avrami, J. Chem. Phys. **7**, 1103 (1939).
[18] B. Wunderlich, *Macromolecular Physics* (Academic Press, New York, 1980), Vol. 2, Chap. 5.
[19] J. D. Hoffman *et al.*, J. Res. Natl. Bur. Stand. Sect. A **79**, 671 (1975).
[20] R. L. Cormia, F. P. Price, and D. Turnbull, J. Chem. Phys. **37**, 1333 (1962).
[21] M. V. Massa and K. Dalnoki-Veress, Phys. Rev. Lett. **92**, 255509 (2004).
[22] F. Gornick, G. S. Ross, and L. J. Frolen, J. Polym. Sci., Part C **18**, 79 (1967).
[23] D. J. Blundell, A. Keller, and A. J. Kovacs, J. Polym. Sci. Polym. Lett. Ed. **4**, 481 (1966).
[24] D. C. Bassett, Polymer **47**, 5221 (2006).